Files

DUMAND NOTE 80-14

DESIGN OF THE SEA URCHIN MODULE
II. Spine Design.

by

D. MCGIBNEY and A. ROBERTS
Hawaii DUMAND Center

This is a progress report on the design of spines for Sea Urchin.

1.0 DESIGN POSSIBILITIES.

Several designs for a simple cylindrical spine are possible:

1. The simplest and cheapest - perhaps the best, in the long run - is a thin glass tube, filled with a low-density solvent with a high index of refraction, in which the WLS is dissolved. The most obvious disadvantage is its fragility.

2. A solid, transparent plastic spine, with the WLS dissolved in the plastic.

3. A solid or tubular transparent base (plastic or glass), with a thin coating of plastic or other transparent resin with the WLS dissolved in it. The coating can be either on the outside, as suggested by Viehmann (1), or the inside, as suggested by Bowen (2).

We will make a comparison of these possibilities later. We must presently note that the cylindrical shape is not necessarily the optimum. It would be better if the outer end of the spine could be flared, so that for the same phase space a larger surface area would be exposed. The degree of improvement available is indicated by the results of the Monte Carlo opacity program discussed below. Such flaring might also be used, at least in principle, to equalize the angular response of the module by appropriate orientation of the flares; at present the module has a considerably greater response at right angles to the diametral plane than parallel to it. (See ref. (3), part I of this paper, hereafter called I, table 3.)

2.0 DESIGN OF LIQUID-FILLED SPINES.

The following variables of the spine have been investigated: Length, diameter, filling solvent, fluor, fluor concentration. To carry out the investigations, the apparatus shown in Figs. 1 and 2 was constructed. It consists of a box in which the spine is exposed to a light source, filtered to duplicate as closely as possible (see Fig. 3) the Cerenkov spectrum expected after Cerenkov light has traversed at least one attenuation length in the ocean. The illumination was made as uniform as conveniently possible, by providing four 8-ft fluorescent daylight bulbs, each covered with a blue filter jacket. One end of the fluorescent spine was coupled optically to a

lucite light pipe which in turn was coupled to a grating spectrometer. The spectrometer measured the output light at an adjustable wavelength by means of a PMT detector . Since the fluorescent light source was strongly modulated at 120 hz, twice the line frequency, a lock-in amplifier tuned to this frequency was connected to the PMT output to provide a sensitive detector of the light output.

The requirement for a suitable fluor is that it have a high quantum yield of fluorescent light; that the absorption spectrum match, as closely as possible, the Cerenkov light spectrum in the ocean; and that the fluorescent light be no redder than necessary to achieve the above objectives. The latter requirement is to ease the difficult problem of finding a photocathode material for detecting the fluorescent light which is highly efficient and not too noisy or too expensive. With the Cerenkov spectrum peaking at about 450 nm, the fluorescent peak will be somewhere around 500 to 540nm, a region in which the more customary phocathodes exhibit rapidly decreasing efficiency.

We have taken extensive data on solutions of these fluors in toluene, at many concentrations; we have also measured their absorption at the mercury line 438 nm. Some of these curves are shown in Figs. 4 to 8. In order to ascertain the attenuation lengths of the fluorescent light, observations were taken in two ways: integral and differential. Integral curves were obtained by covering all the spine except the first L cm (nearest the PMT), and varying L. Differential curves were obtained by exposing a length of L cm along the spine, and varying the position of the exposed region with respect to the detector.

In addition to readings taken with the grating spectrometer, in which one can observe the change of the spectrum shape as the length of attenuator is varied, it has also been useful to take data in which the spectrometer is replaced by a PMT. In that case the observation measures the quantity that is physically the most significant: the integrated response to the fluorescence spectrum by the PMT. In our case we used a PMT with a tri-alkali (S-20) wide-band response. It is significant that it was in these data that the deviations from a single attenuation length were most marked.

2.1 Results

Fig.4 shows a collection of response spectra from a wide variety of fluors. The solvent was usually toluene, but sometimes alcohol. The curves have not been corrected for PMT response, but are weighted by the S-20 sensitivity. The variation of sensitivity of the S-20 cathode is also indicated.

All these curves were taken with the same sample cell, a 60-cm long, 1/2 " diameter glass tube, and at the same sensitivity settings, so that the responses are directly comparable.

Figs. 5 to 7 show spectra of several fluors as a function of concentration, all for the same sample cell. Fig. 8 shows how the fluorescent spectrum changes with attenuation; this is the origin of the deviation from a single attenuation length mentioned above.

Fig. 9 is a study of the attenuation of Hostasol Yellow 8G, (and Fig. 10 for Hostasol Yellow 3G), as measured at a single wavelength at the peak of the spectrum. Curves are shown for several different concentrations. It is noteworthy that maximum response is achieved at a wavelength where the radius of the tube is 2 or 3 attenuation lengths for the incident light. Finally, Fig. 11 shows the same attenuation measurements, but made without the spectrometer; the entire spectrum is integrated by the PMT.

2.2 Discussion of Results.

The usefulness of the concept of attenuation length as applied to the fluorescent spectrum deserves some comment. Figs. 9 and 10 illustrate that the attenuation of a single wavelength near the peak of the spectrum behaves closely as a simple exponential; the concept of attenuation length is clearly applicable. Figs. 11 and 12, taken without a spectrometer, show a totally different behavior, which cannot be described so simply. For 50 mg/l concentrations of Hostasol 8G, the slope in Fig. 11 changes from one corresponding to an attenuation length of 1.16m at the beginning to a value of 5.6m after two meters. In Fig. 12, for 3G, it goes from 1.68m to 4.0m.

One can introduce the concept of incremental attenuation length, the value corresponding to the slope at any position; this is useful for setting a minimum value for use in considering extending the spine length. But it is clear that one cannot calculate the total light obtained from a spine just from a single reading and an attenuation length. This subject will require further study.

The data make it apparent that the best fluors, from the standpoint of both light output and cost, are the two Hostasol Yellows. The final choice between them may depend upon the type of photocathode chosen for the PMT, since the cathode efficiency varies rapidly in this region, as shown by the data in Table 1.

Table 1. Comparison of Measurements with Different PMT's.

The following data were taken with 50 mg/l solutions of Hostasol Yellow 3G and 8G in an 8-ft long glass tube. Data from different PMT's are not to the same scale.

PMT	Spine Filling: Hostasol Yellow	
	8G	3G
56AVP (S11A cathode)	40 mV	33 mV
150CVP (S20 cathode)	40	47.5

3. ALTERNATIVE SPINE DESIGNS.

3.1 Thin WLS Coating on Transparent Rods or Tubes.

Proposals have been made by Viehmann et al. (1) and by Bowen (2) for spines in which the WLSA is deposited in a concentrated solution in a thin coat of transparent plastic or resin, on either the outside surface of a rod, or the inner surface of a tube. In order for these designs to be feasible, the attenuation of the solid material of the rod or tube would have to

be comparable to that of the toluene- filled glass tube design. Viehmann's figures indicate that this condition is not fulfilled, or even approached, with either PMMA or fused silica (which is very expensive.) Consequently we hold out little hope for this technique for our application.

3.2 Transparent Plastic Spines.

A solid spine, even if brittle, appears to offer fewer hazards of self-destruction in manufacture, deployment, and operation, than a liquid-filled glass spine. It offers an attractive possibility, therefore, if it should be feasible, to get rid of both the fragility and the potential environmental hazard posed by the organic liquid filling. We have therefore investigated plastic spines to some depth. Unfortunately, the results do not look encouraging.

3.21. Materials. Only two major posibilities for base plastics are available (with some variants.) They are acrylic resins (PMMA) and polystyrene. Table 2 shows their relevant properties. One module would use about 1100 10-ft 1/2" spines.

TABLE 2. Properties of PMMA and polystyrene spines.

PLASTIC	DENSITY	INDEX OF REFRACTION	COST/FT OF 1/2 INCH ROD	COST/MODULE (1170 X 10 FT)
Acrylic (PMMA)	1.16-1.20	1.48	.80	$9360
Polystyrene	1.05	1.595	.28 (.15	3276 1755)

The cost of the acrylic is for cast and polished rod. Some reduction for very large quantities is possible, but not enough to compete with toluene or styrene. The cost of polystyrene is for extruded rod, since cast rod is impractical and unavailable. Extruded rod requires polishing. The figure 0.28/ft is a current commercial quotation for large quantities (1000 lb.) The .15/ft figure is from another commercial firm experienced in extrusion, but not with polystyrene, and represents a guess as to a possible long-term asymptotic cost. It is listed as a best possible alternative in case the liquid-filled spines, for any reason, may have to be rejected. However, it is not yet clear that extruded polystyrene will have the desired transparency.

4. EFFICIENCY OF THE SEA URCHIN SPINE AS A LIGHT TRANSFORMER

The detailed course of the physical process whereby incident Cerenkov light, predominantly in the blue, is transformed in the spine to yellow-green and collected at the PMT photocathode, can be traced in detail and simulated by a Monte Carlo program. This is done, to a good approximation, in the program CYL6X, written by A. Roberts, which simulates most of the processes occurring. In detail, it does the following:

1. Incident light uniformly distributed along the spine is assumed. It is averaged over all angles of incidence, weighted by the cosine of that angle. At each angle of incidence the amount reflected and the amount transmitted are calculated, and the direction of the refracted ray found. A

coefficient of attenuation of the incident light in the medium is given as data, and the source function for the fluorescent light is found by making it proportional to the primary light absorbed in each element of track length. The final result is stored in an array which represents the source function.

2. The fluorescent light is assumed to be isotropically emitted, with an intensity given by the source function.

3. The fluorescent light is now examined to see how much of it is captured by internal reflection. The propagation down the spine is characterized by a coefficient of attenuation for the fluorescent light, and a surface reflection coefficient that simulates surface imperfections. Light propagating away from the PMT is assumed to be reflected at the end of the spine.

The chief remaining fault in the simulation is the simplification of the incident and fluorescent light interactions with the medium. It is described in each case by a single attenuation coefficient. For the incident light that approximation is good; it amounts to averaging over a range of absorption coefficients rather than using a single fixed value, in a range where the absorption changes slowly. In the case of the emitted light, however, there are complications. The emitted light spectrum and the incident light spectrum overlap; the effect of this is to make the overlap region disappear quickly, since emitted light in that range is quickly reabsorbed. In addition the self-absorption varies relatively rapidly over the remainder of the spectrum. Thus the mean absorption coefficient is not a constant. Experimentally, a plot of the differential absorption shows this curvature distinctly (see, e.g., Fig.11)

Consequently the program is still an approximation; however, it is a sufficiently good one so that it is useful. It enables us to compare and evaluate different situations.

4.1 Predictions of the CYL6X Program.

Fig. 13 shows the variation of the total intensity with the attenuation length of the incident light in the solution. The two curves indicate respectively total light, and light within a fixed exit cone angle (which is what is actually utilized.) Fig. 14 indicates the variation of attenuation length with each of the two variables that control it in a glass spine: the absorption coefficient of the solution, and the surface reflection coefficient (SR) of the glass. The bulk attenuation (denoted by alpha) is independent of the spine diameter; but surface reflection losses decrease with increasing radius, because there are fewer reflections per unit length. Since the SR is total internal reflection, the losses are due entirely to surface imperfections. Figs. 15a and 15b show the variation of attenuation length, first with SR for fixed alpha, then vice versa. Figs. 16a and b show the angular distribution of the light emerging from the end of the spine as a function of SR for no attenuation, and for a fixed moderate absorption, respectively. The larger the total attenuation, the more parallel the output light.

Using this program, we have investigated the effect of various parameters on the efficiency of the spine. In particular it has been possible to find the

incremental value of an increase in the index of refraction of the solvent, the importance of parameters like the surface reflection coefficient, the attenuation coefficient of the incident light, etc. It was also possible to search for values of the coefficients yielding results that simulate the measured values found with real spines in the laboratory. To date it has not been possible to test the predictions in detail.

5. SPINE COSTS.

We now consider the cost of spines in some detail, because there is a choice of several possibilities, and design optimization will depend strongly on cost.

As described in Sec. 1, there are three spine designs that have been considered.

1. Glass spine with fluor in solution
2. Plastic spine, with fluor in (solid) solution.
3. Tubular spine, with fluor deposited in solution in a thin film of plastic on the outer or inner surface.

From all available information, and from preliminary tests performed in our laboratory, plastic tubes are both too expensive and too opaque for our use; and fused silica, which is more transparent, is far too expensive (over $10/lb.) Consequently Alternative No. 3 can be immediately ruled out on the basis of cost.

The elements of cost in No. 1 can be listed as follows:

1. Glass Tube
   a. Tube itself
   b. End Windows.

2. Filling.
   a. Solvent.
   b. Fluor.

3. Termination (Pressure equalizing seal.)
   a. Materials.
   b. Assembly

4. Assembly and Filling.

Since the possible terminations have not yet been tested, our attention will have to be concentrated on other areas. Up to now we have been almost entirely concerned with finding the optimum dimensions and filling of the spines; without a design of adequate sensitivity and acceptable cost, the other problems never arise.

5.1 Fluorescent Solution.

We first consider in detail the choice of fillings available to us. The desirable characteristics of the filling are low density, high index of refraction and low cost. Also important is low toxicity, particularly respiratory, since we will be handling very large quantities a little at a

time. For deployment in the ocean, its environmental effects in the event of spills should be tolerable.

5.11 Fluor. The cost of the filling includes both solvent and fluor. We find that as the diameter of the spine increases, the optimum concentration of the fluor drops, so that the amount of fluor needed does not depend strongly on spine diameter. It now appears that one module may use about 600 liters of solvent; at a concentration of 25-50 mg/l, this requires a total of 15 to 30 gm of fluor per module. Fluor costs range from pennies per gram to $75/gm. Thus some fluors would be ruled out on the basis of cost. Fortunately, the best fluors we have found, Hostasol Yellow 3G and 8G, are very inexpensive.

5.12 Solvent. The solvent cost is important; if the spine cost is to remain under the desired $400/module, the cost per liter must not exceed .33, if half the cost is to be reserved to the glass tube and the termination. That is just about the current cost of gasoline. However, aliphatic hydrocarbons and alcohols all have excessively low indices of refraction, not much greater than that of water. Aromatics are much better. The cheapest, benzene, unfortunately has a melting point of 15C at 500 atmospheres pressure. Other possibilities are toluene, styrene, xylene, and related compounds like aniline, ethyl benzene, and benzyl alcohol. The requirements of low density (appreciably less than water) and high index of refraction (above 1.50) rule out some of these and most others; The requirement of low cost singles out toluene uniquely, with styrene some distance behind. The cost of toluene is about that of gasoline; styrene costs about twice as much. Table 3 shows the properties of these two leading contenders.

Table 3. Comparison of Styrene and Toluene.

The values quoted are for a pressure of 500 atmospheres (equivalent to a depth of 5km.)

LIQUID	DENSITY	INDEX OF REFRACTION	RELATIVE LIGHT COLLECTION	COST/ LB.
Toluene	0.90	1.51	1.00	$.214
Styrene	0.93	1.56	1.22	.38

Toluene is only mildly toxic (as inhalant; we do not consider ingestion.) It is readily available in tank-car and even shipload quantities. It does not need to be specially purified (we are told) since its principal impurities are not harmful for our uses; they are mostly benzene, xylene, and related aromatics. Oxidants like sulphur would be harmful if present. It is a solvent for most of the fluors we are interested in. The Hostasol Yellows require encouragement with a percent or so of alcohol.

5.13 Glass tube. This leaves the glass tube for consideration. At this time we do not have complete information on the possibilities; we are in process of collecting it. We base present calculations on data from Sylvania Glass Co, with the warning that since that company cannot offer us tubes in excess of 8 ft in length, the numbers will probably need revision. Nevertheless, they will prove instructive. We use the Sylvania quote of $.269 per 8-ft length of 1" diameter tubing of soda-lime glass, density 2.47, wall thickness .66mm.

The following table is based on a comparison of 12-ft spines of 1" diameter, with packing fraction 0.7, and 1/2" spines 10 ft long, with packing fraction 0.5, since from Fig. we can see that these have the same effective area, and thus the same sensitivity.

Table 4. Preliminary cost comparison, 12-ft 1" and 10-ft 1/2" Spines. This does not include the cost of end windows on glass tubes or of pressure terminations.

Glass.

12-ft 1" D. Cost .269 x 1.5 = .403 Cost of 404 tubes = $163.01
10-ft 1/2" D. Cost .135 x 1.2 = .162 Cost of 1156 tubes = $187.27

Toluene.

We assume the cost of toluene is $1.60/gallon, or .424/liter; at 500 atmospheres, a density increase of 2.5% makes this .435/1.
12-ft, 1" D.: 1.670 lx.435/1 x 404 spines = 674.61 for $293.22
10-ft 1/2"D.: .310 1 x.435/1 x 1156 spines = 358 1 for $155.89

Net Buoyancy. Cost of Buoyancy $4/kg.

12-ft 1" Tube: Wt in water 270.3 gm. Buoyancy of toluene 225.45 gm.
Net Wt. per Spine: 44.85 gm x 404 spines = 17.94 kg total Wt.
10-ft 1/2" Tube: Wt in water 109.42 gm. Buoyancy of toluene 41.88 gm.
Net wt. per Spine 67.54 gm; x 1156 spines =78.1 kg total wt.
Cost to provide neutral buoyancy: 17.94 x 4 = $71.76, for 1" spines.
Cost to provide neutral buoyancy: 78.1 x 4 = $312.32, for 1/2" Spines.

Summary of Costs.

	1" Spines	1/2" Spines
Cost of Glass	$163.01	$187.27
Cost of Toluene	$293.22	$155.89
Cost of Buoyancy	71.76	$312.32
TOTAL	$527.99	$655.48

5.2 Alternative Designs.

The second alternative, plastic spines, admits only two practical possibilities: acrylic and polystyrene. Acrylic is not only much too expensive (over $5 per 1/2" spine), but has a high density (1.15 to 1.20) and a low index of refraction (1.48). Polystyrene is less transparent than acrylic; we are in process of obtaining measurements on it now. Its density is 1.05, making it almost neutrally buoyant, and its index of refraction is 1.595, which is extremely good. It would increase the light collection about 30%. Polystyrene transparent rods must be extruded, not cast; and the finish on extruded rods is not good enough for our purposes.

However, overriding all technical problems is the matter of cost. The only firm quotation we have on polystyrene rods is at .28/ft for 1/2"-inch rod, making a single 10-ft spine cost $2.80; thus 1156 spines would cost over $3000. Unless we can find a much cheaper source, this looks unpromising. The raw plastic is only about $.60/lb, and the rest of the cost is the extrusion process. We postpone further discussion for the present.

6. CALCULATION OF THE EQUIVALENT AREA OF THE SEA URCHIN.

The equivalent area E of a Sea Urchin module can be calculated from the two Monte Carlo programs described above, and the observed attenuation length of the light from the spine. The equivalent area can be defined as follows:

$$E = GA \times \eta(d, PF) \times \varepsilon(N1, N2, c, L, A) \times FE \times \beta$$
$$= EA \times \varepsilon \times FE \times \beta$$

where

GA = geometric area of the module, area of circle of radius spine length plus radius of glass sphere.
$\eta(d, PF)$ = efficiency factor for opacity as a function of spine diameter d and packing fraction PF (from I, Fig. 7),

EA = effective area, product of the above two factors,

$\varepsilon(N1, N2, c, L, A)$ is the collection efficiency for fluorescent light of the spine; it is a function of the indices of refraction of the water N1, the solvent N2, of the fluor concentration c, the length L, and the incremental attenuation length A.

FE = fluorescent efficiency of the fluor,

β = correction factor for light outside the accepted cone angle, and other possible losses, e.g. optical contact, etc.

For example: with d = 1", L = 3.66m (12 ft), A = 3.85m (measured for Hostasol 3G), N1 = 1.35, N2 = 1.51 (toluene), we find:
GA = 47.05 sq.m.
EA = 16.5 sq.m. (From I, Fig. 7)
ε = 0.098 (from CYL6X),
β = 0.8

We obtain E = 1.08 sq.m., for vertically incident light. For light incident from the side, Table 2 of I gives EA = 12.7 sq.m., or 0.77 as much; thus E becomes 0.83 sq.m.

An incident light flux of 50 quanta/sq.m. and 10% photocathode efficiency would yield 5.4 and 4.2 photoelectrons respectively.

REFERENCES

1. W. W. Viehmann and R. L. Frost, "Thin Film Waveshifter Coatings for Fluorescent Radiation Converters," NASA Technical Memo 79723, 1979.

2. T. Bowen, "A Glass Pipe Inductively-Coupled DUMAND Photodetector Module", Univ. of Arizona, Tucson (unpublished)

3. "The Sea Urchin Module. I. Survey of Design Problems", by D. McGibney, A. Roberts, and U. Camerini, Hawaii DUMAND Center; DUMAND Note 80-13, 1980; to be published in Proc. of 1980 DUMAND Summer Symposium-Workshop. (Hereafter referred to as I.)

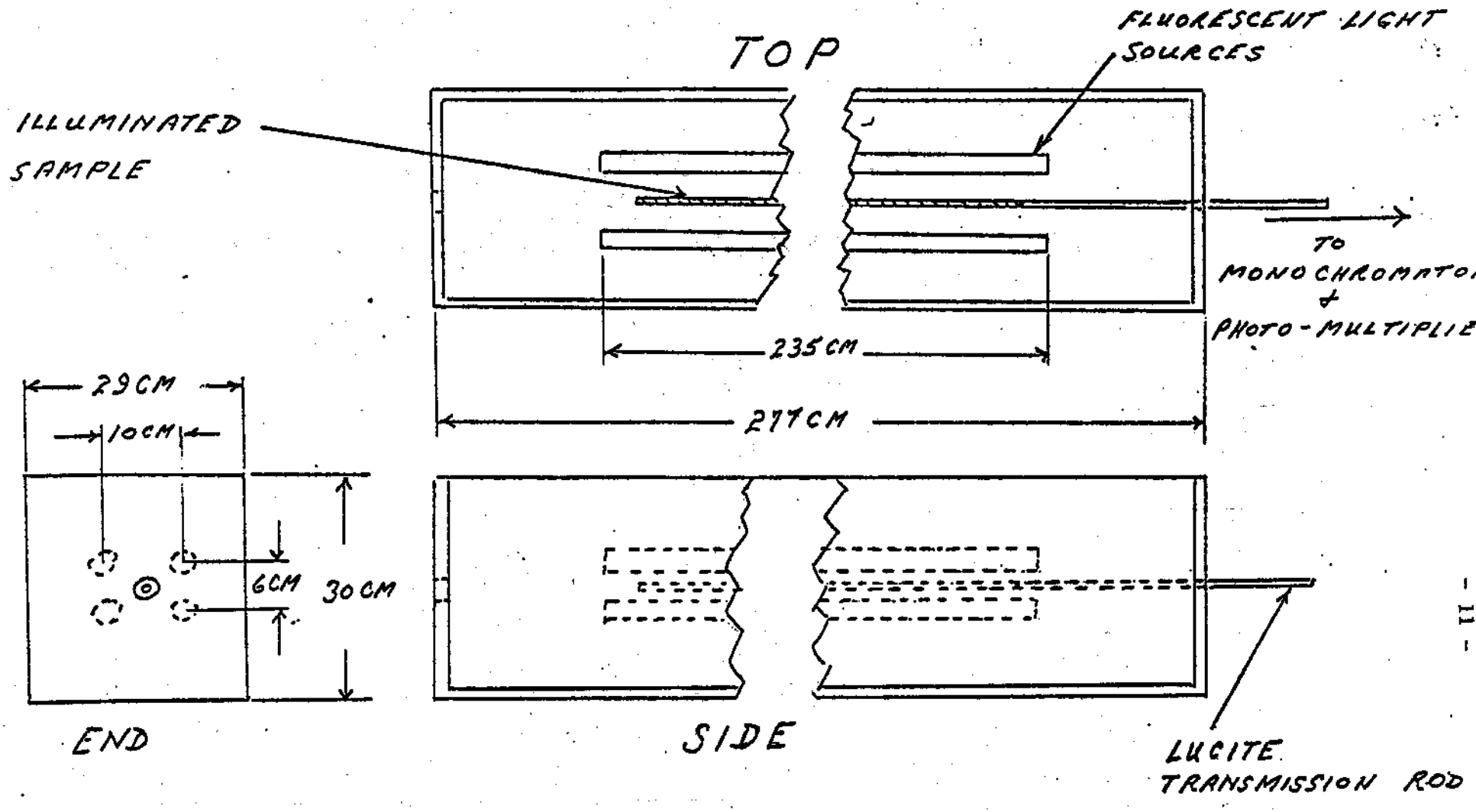

FIG. 1 DETAILS OF LIGHT BOX USED TO EXPOSE SPINES TO SIMULATED CERENKOV SPECTRUM IN WATER

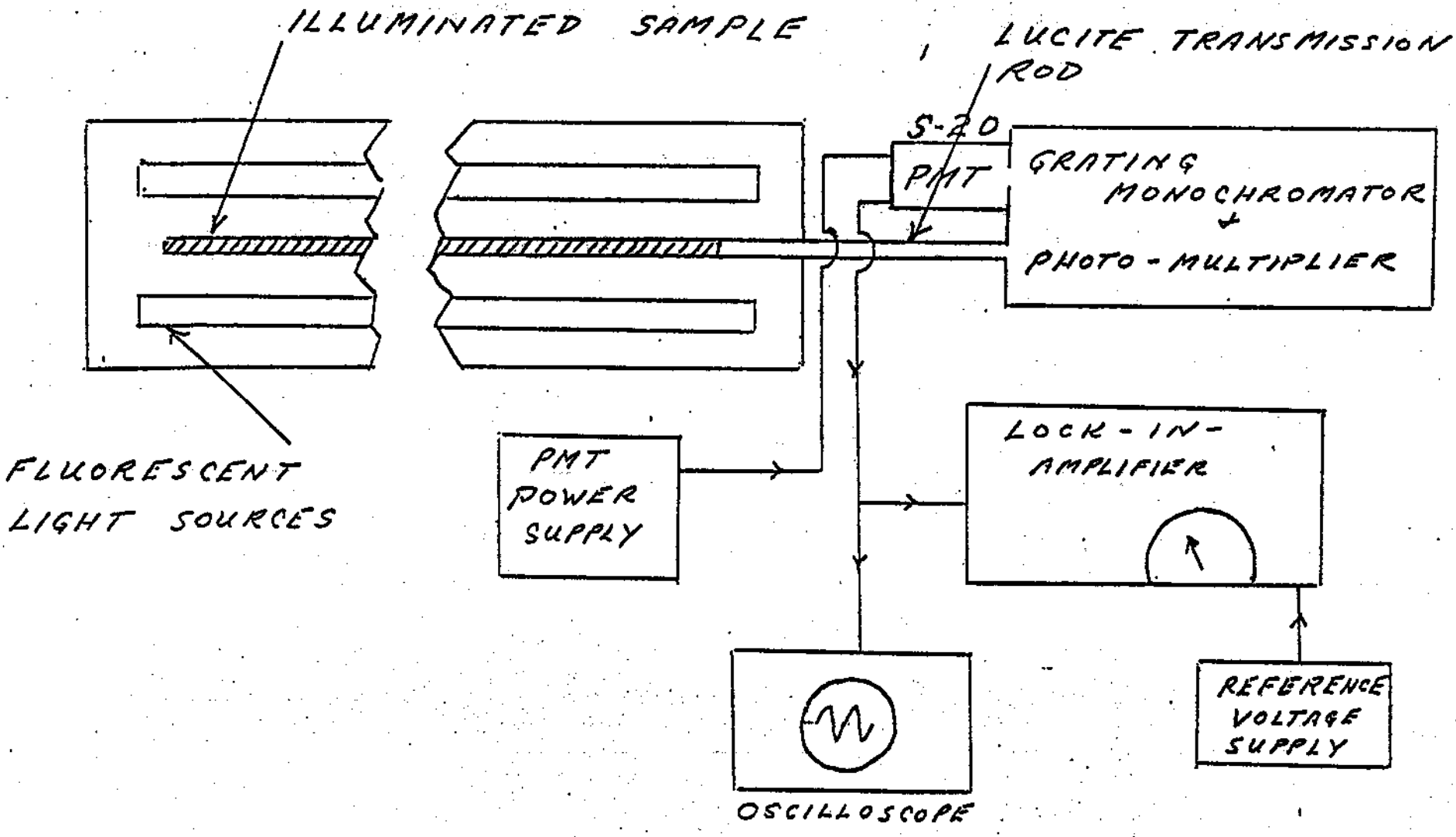

FIG. 2 EXPERIMENTAL APPARATUS FOR MEASUREMENT OF FLUORESCENCE SPECTRA

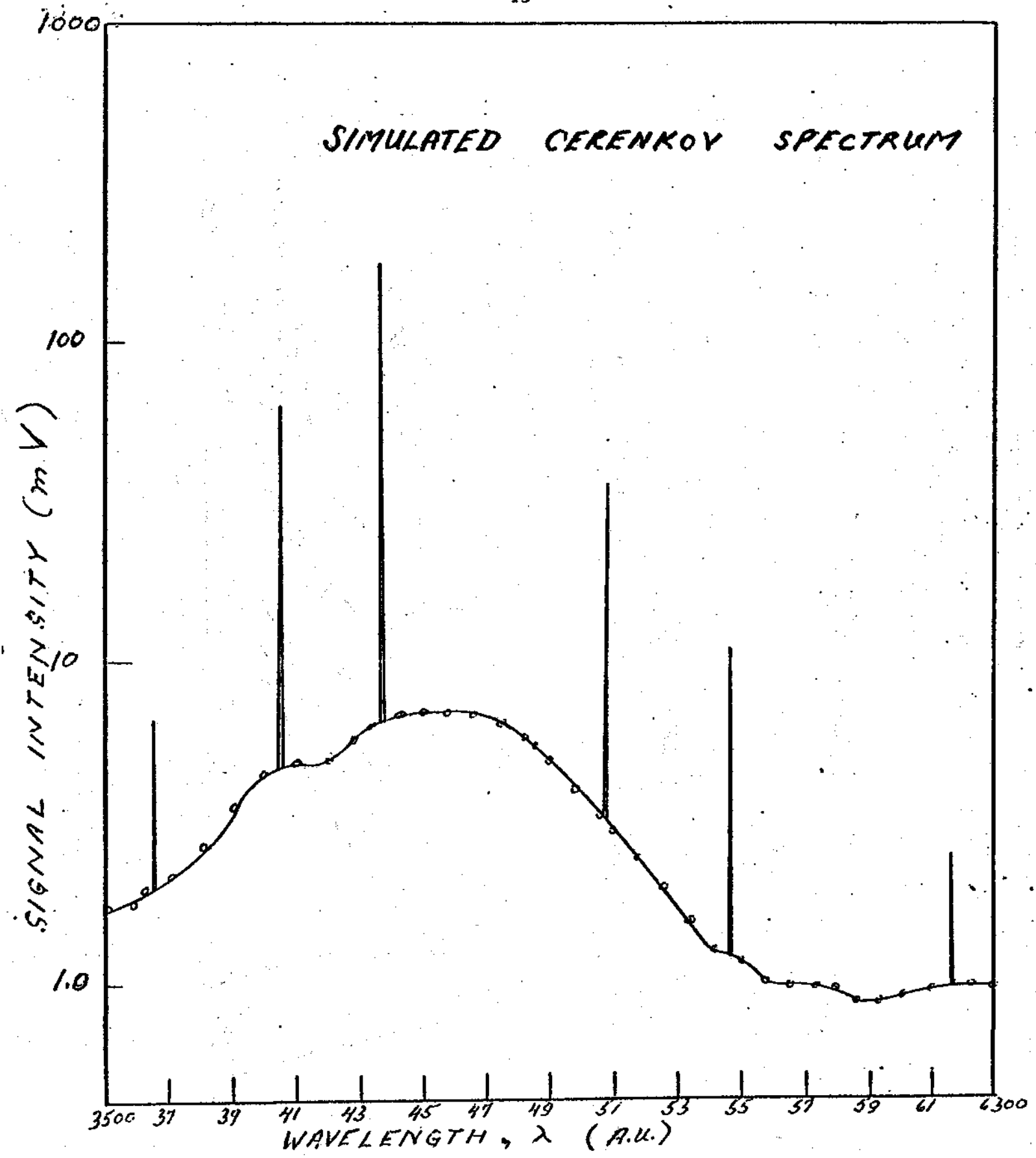

Fig. 3. The simulated Cerenkov spectrum obtained by filtering the "cool white" fluorescent tubes with jackets of the theatrical gel filter "Brilliant Blue". The line spectra shown superposed on the continuum are very narrow (1-2 A.U.) and contain less than 5% as much light as the continuum.

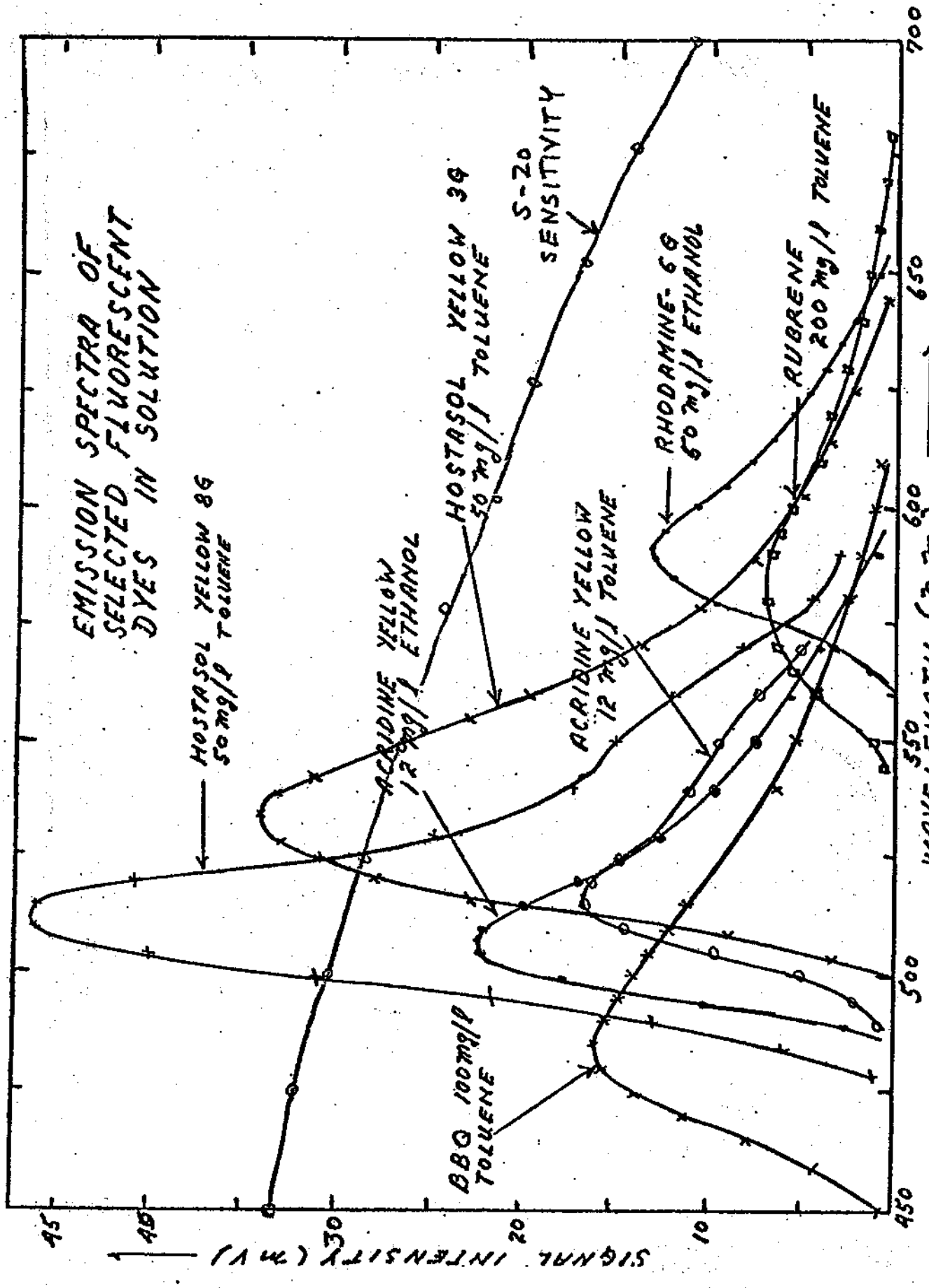

Fig. 4. Summary of the observed fluorescent spectra of some representative fluors illuminated with the Cerenkov spectrum of Fig. 3. All observations were made with the same light source, intercalibrated gain settings, and using the same sample tube and geometry, and are thus directly comparable. The PMT used had an S-20 photocathode, but no correction has been made for its variation in sensitivity, which is shown in the superposed curve. Unless labelled otherwise, [illegible]

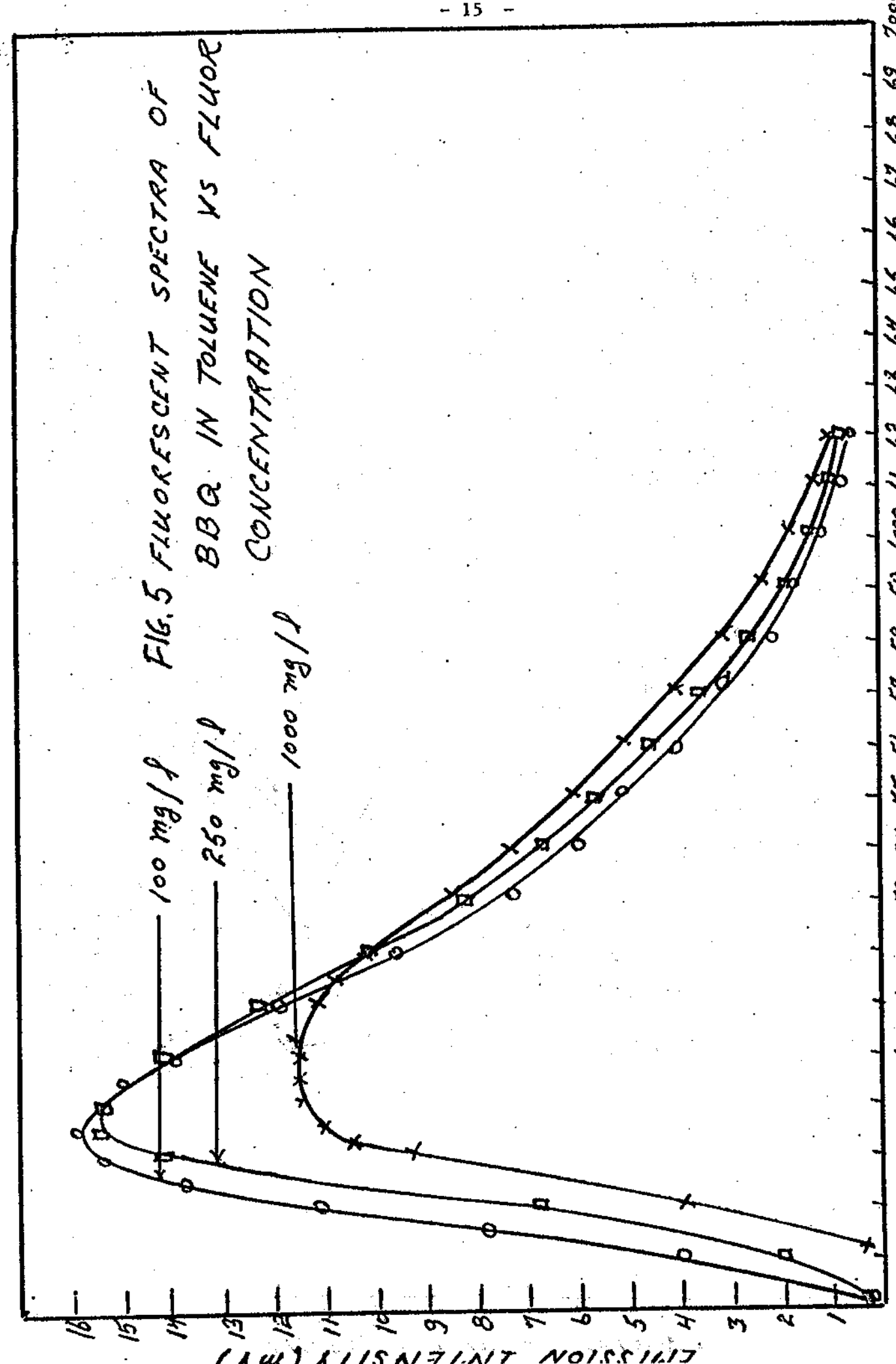
FIG. 5 FLUORESCENT SPECTRA OF BBQ IN TOLUENE VS FLUOR CONCENTRATION
100 mg/l
250 mg/l
1000 mg/l
EMISSION INTENSITY (mV)
WAVELENGTH, λ (A.U.)

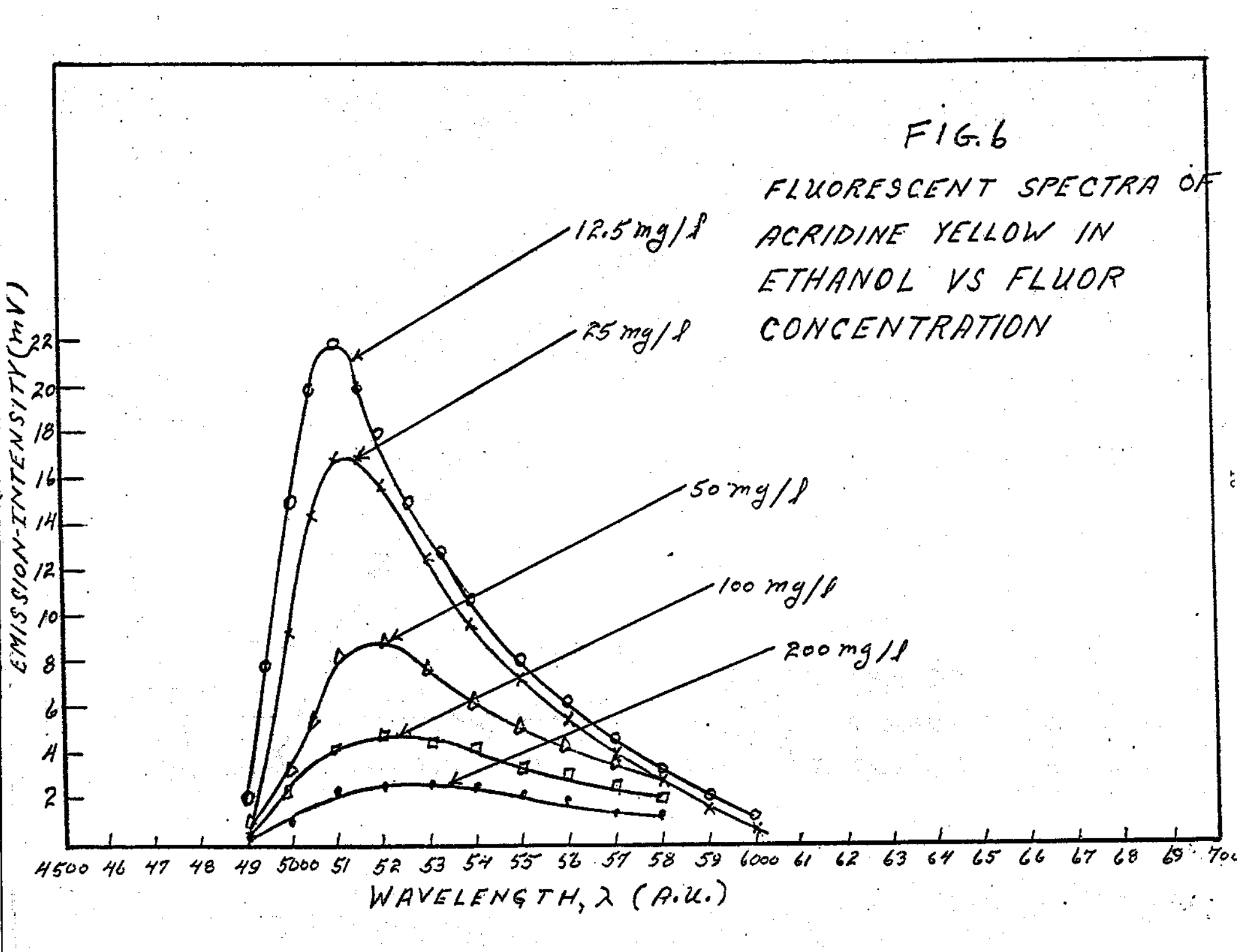
FIG. 6
FLUORESCENT SPECTRA OF ACRIDINE YELLOW IN ETHANOL VS FLUOR CONCENTRATION
12.5 mg/l
25 mg/l
50 mg/l
100 mg/l
200 mg/l
EMISSION-INTENSITY (M)
22
20
18
16
14
12
10
8
6
4
2
4500 46 47 48 49 5000 51 52 53 54 55 56 57 58 59 6000 61 62 63 64 65 66 67 68 69 70
WAVELENGTH, λ (A.U.)

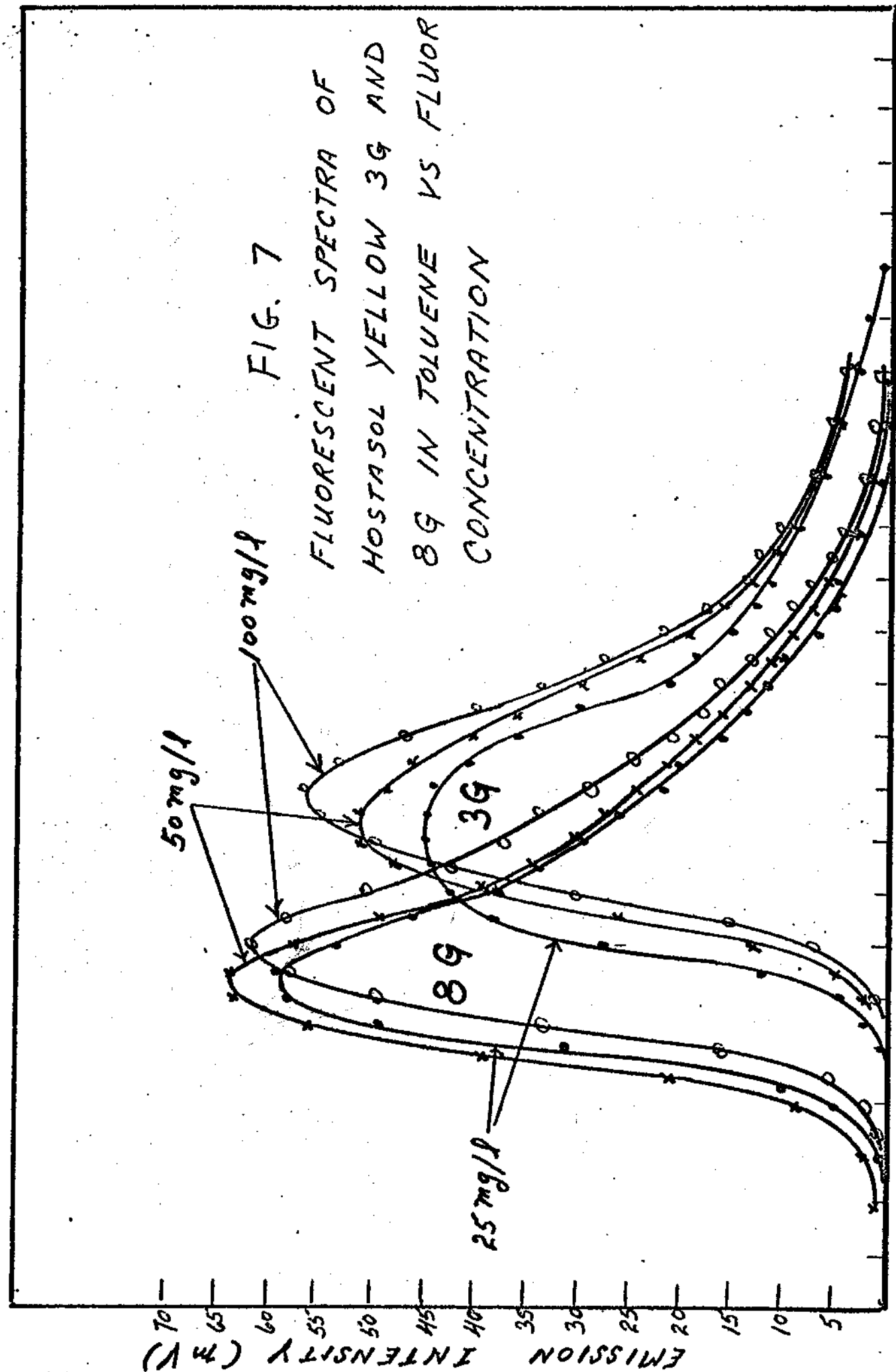
FIG. 7
FLUORESCENT SPECTRA OF HOSTASOL YELLOW 3G AND 8G IN TOLUENE VS FLUOR CONCENTRATION
100 mg/l
50 mg/l
25 mg/l
3G
8G
EMISSION INTENSITY (mV)
WAVELENGTH, λ (Å)
70 65 60 55 50 45 40 35 30 25 20 15 10 5
4500 4600 4700 4800 4900 5000 5100 5200 5300 5400 5500 5600 5700 5800 5900 6000 6100 6200 6300 6400 6500 6600 6700 6800 6900

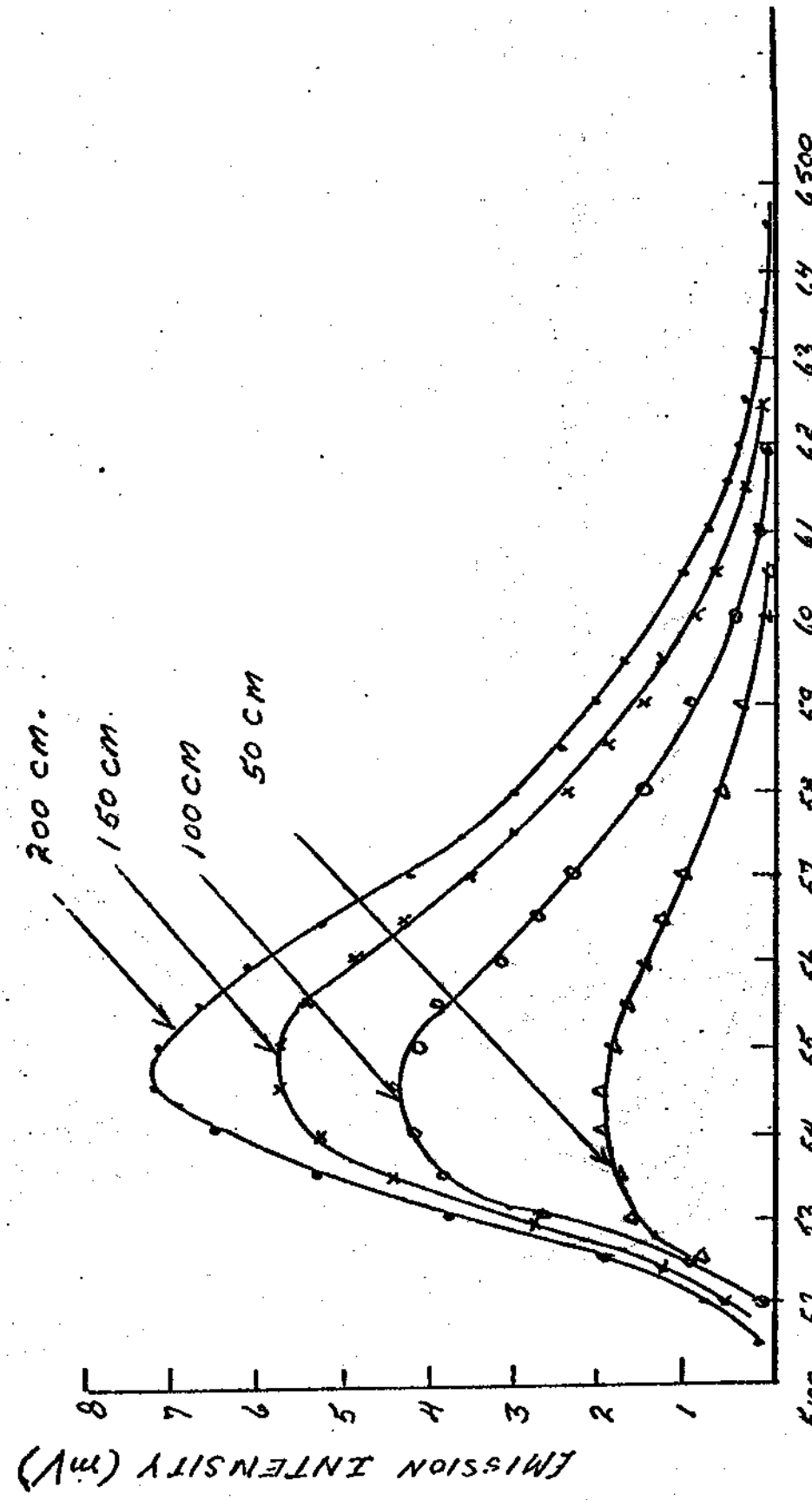

Fig. 8. The change in spectrum due to attenuation in the spine: the spectrum of Hostasol Yellow 3G from spines of different lengths.

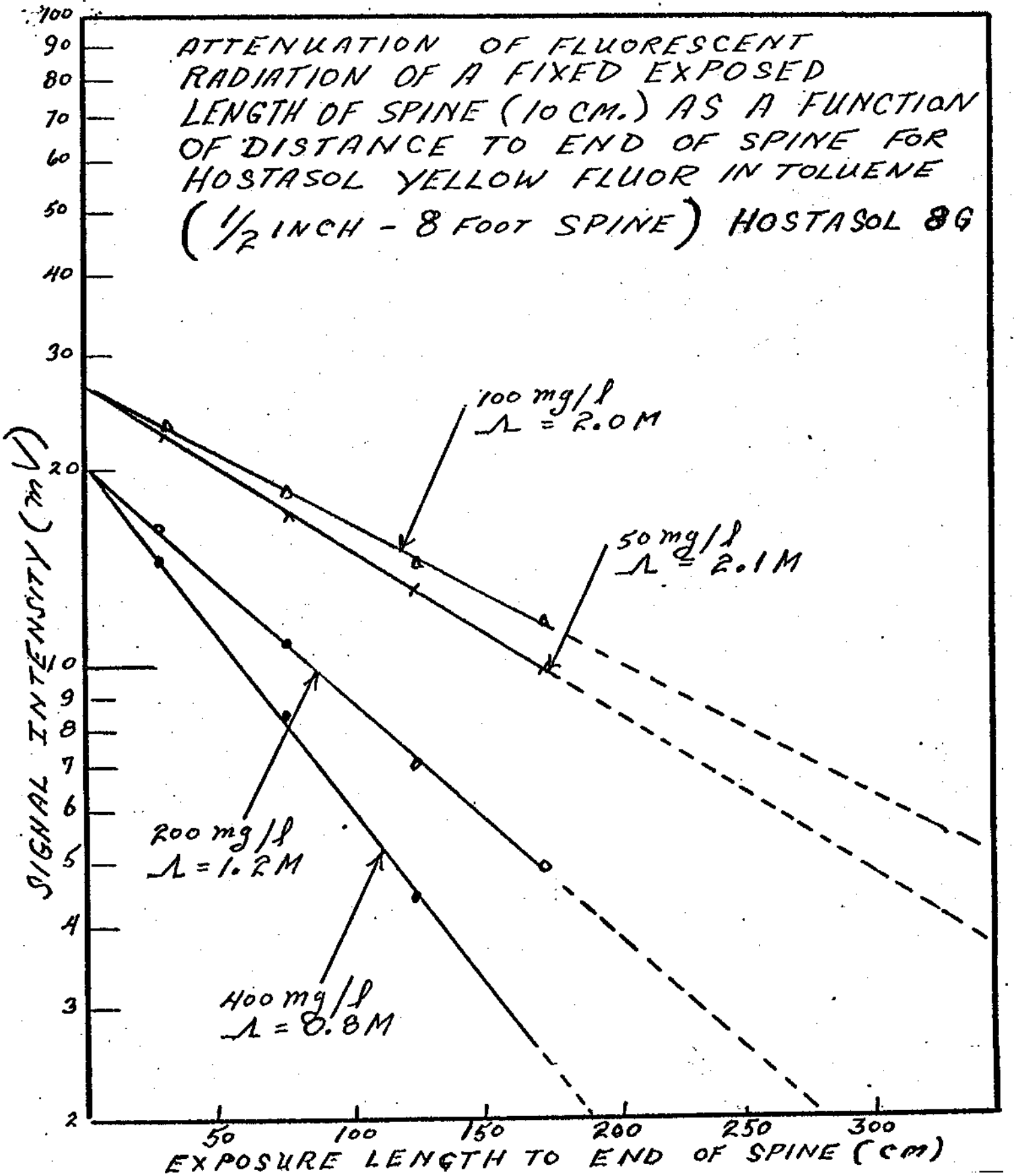

Fig. 9. Measurement of attenuation of fluorescent radiation using the spectrometer as in Fig. 2. This is a differential curve, showing the intensity from a fixed length L as a function of the distance between L and the end of the spine; measurements all being at the same wavelength. Data are for Hostasol Yellow 8G.

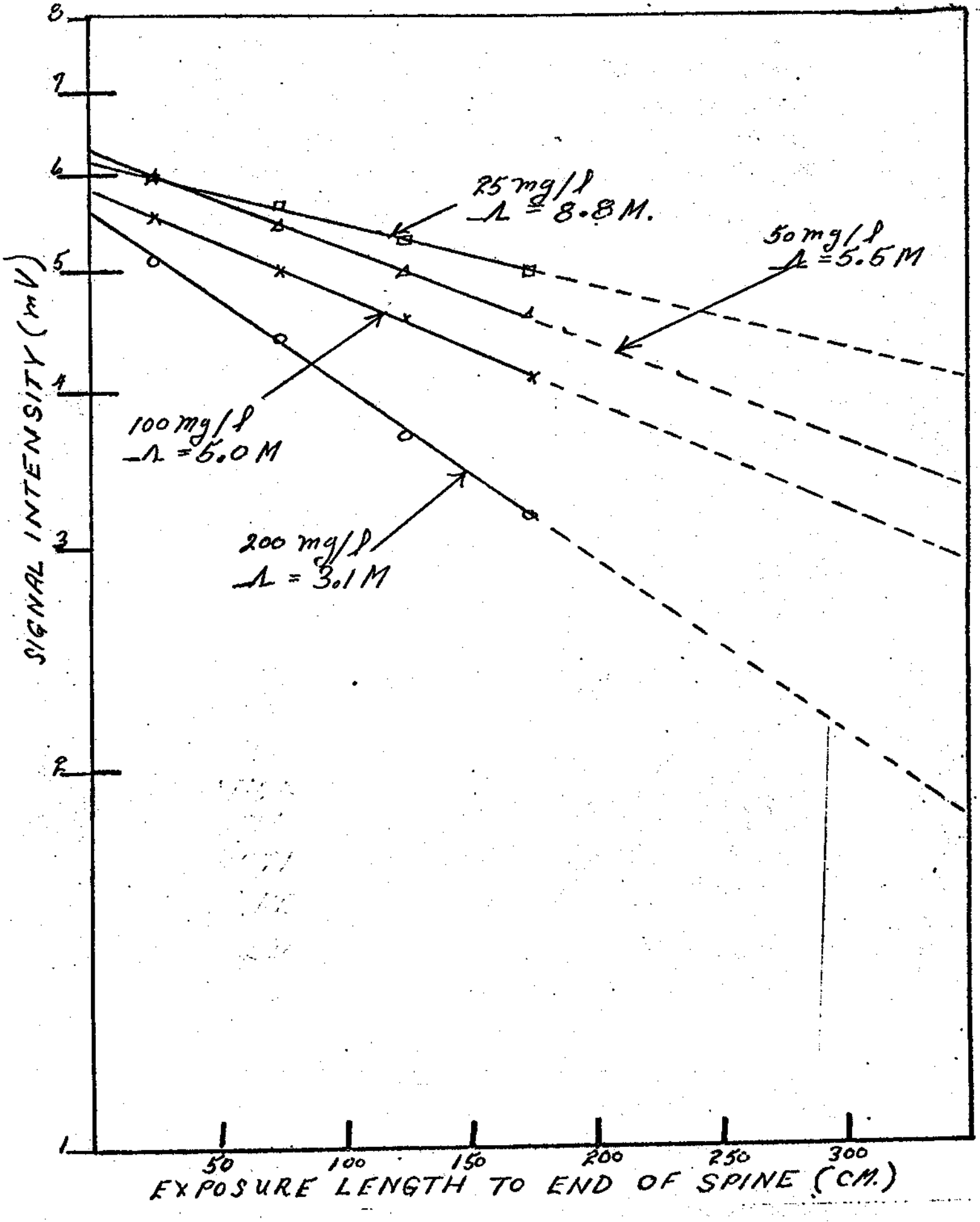

Fig. 10. Same as Fig. 9, but for Hostasol Yellow 3G.

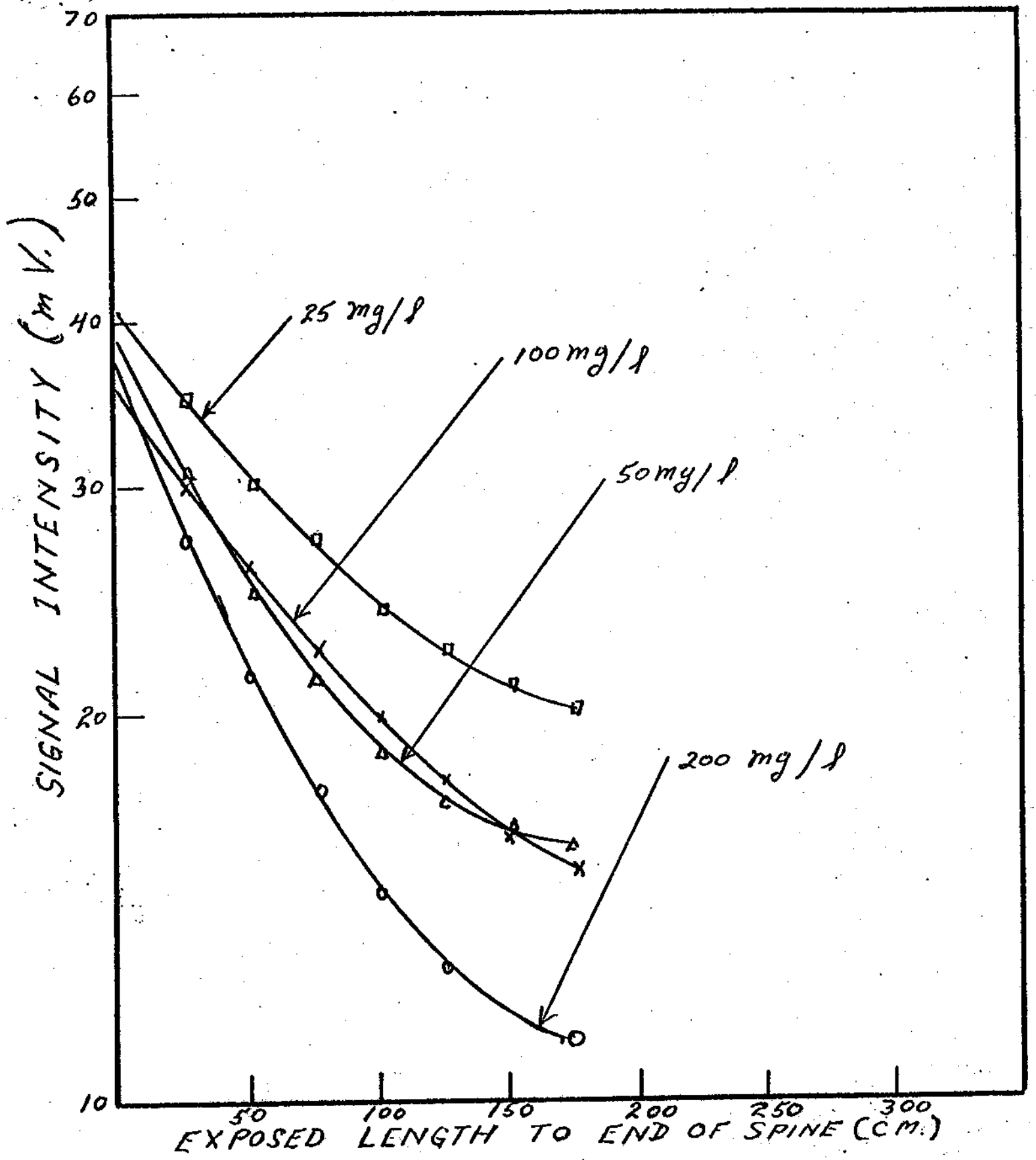

Fig. 11. Attenuation curve like that of Fig. 9, for the same fluor, but taken without the spectrometer: thus the entire spectrum is observed at once, and the attenuation measured is that of the signal integrated over the whole spectrum. Note the much greater deviation from exponential attenuation.

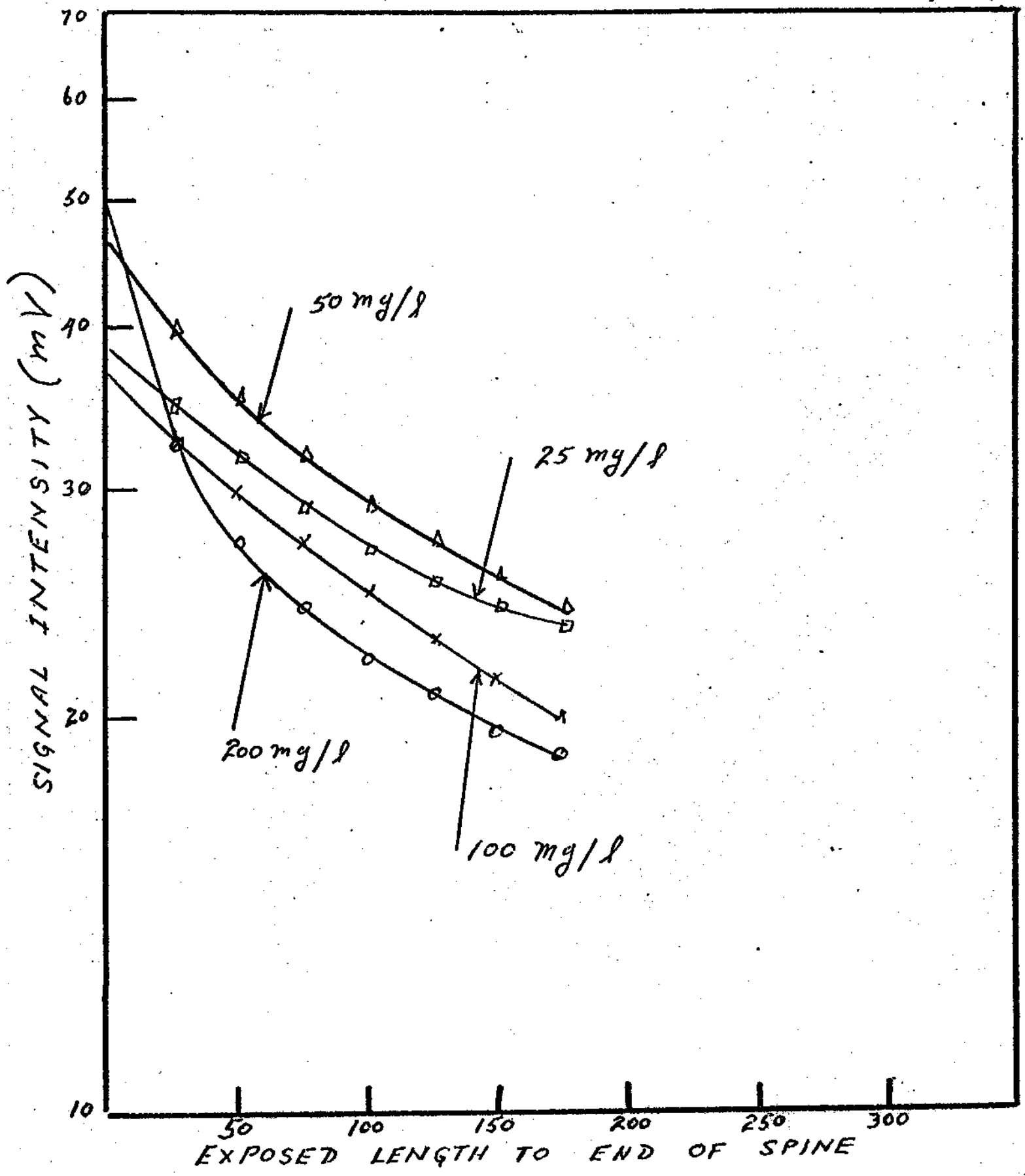

Fig. 12. Same as Fig. 11, for Hostasol Yellow 3G.

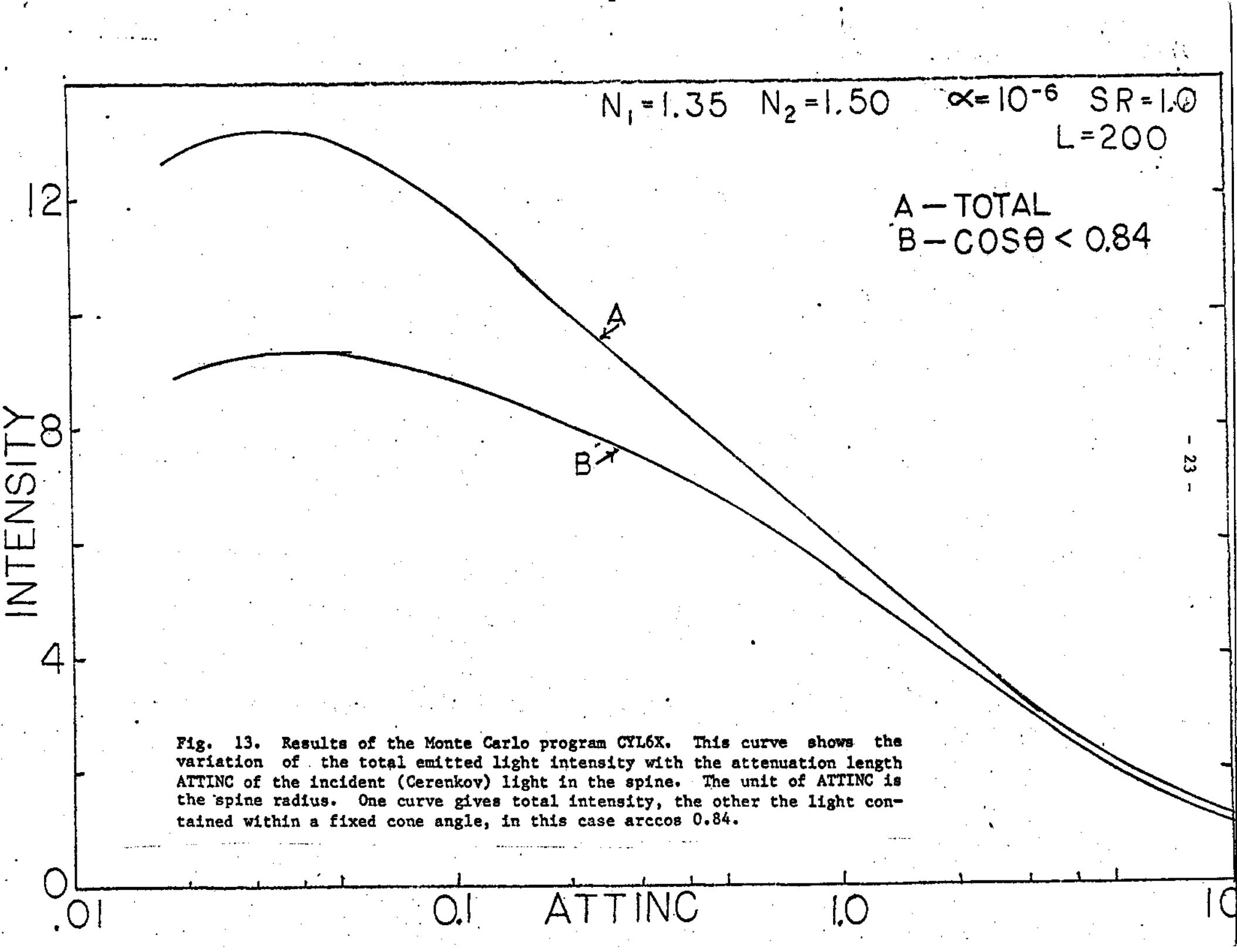

Fig. 13. Results of the Monte Carlo program CYL6X. This curve shows the variation of the total emitted light intensity with the attenuation length ATTINC of the incident (Cerenkov) light in the spine. The unit of ATTINC is the spine radius. One curve gives total intensity, the other the light contained within a fixed cone angle, in this case arccos 0.84.

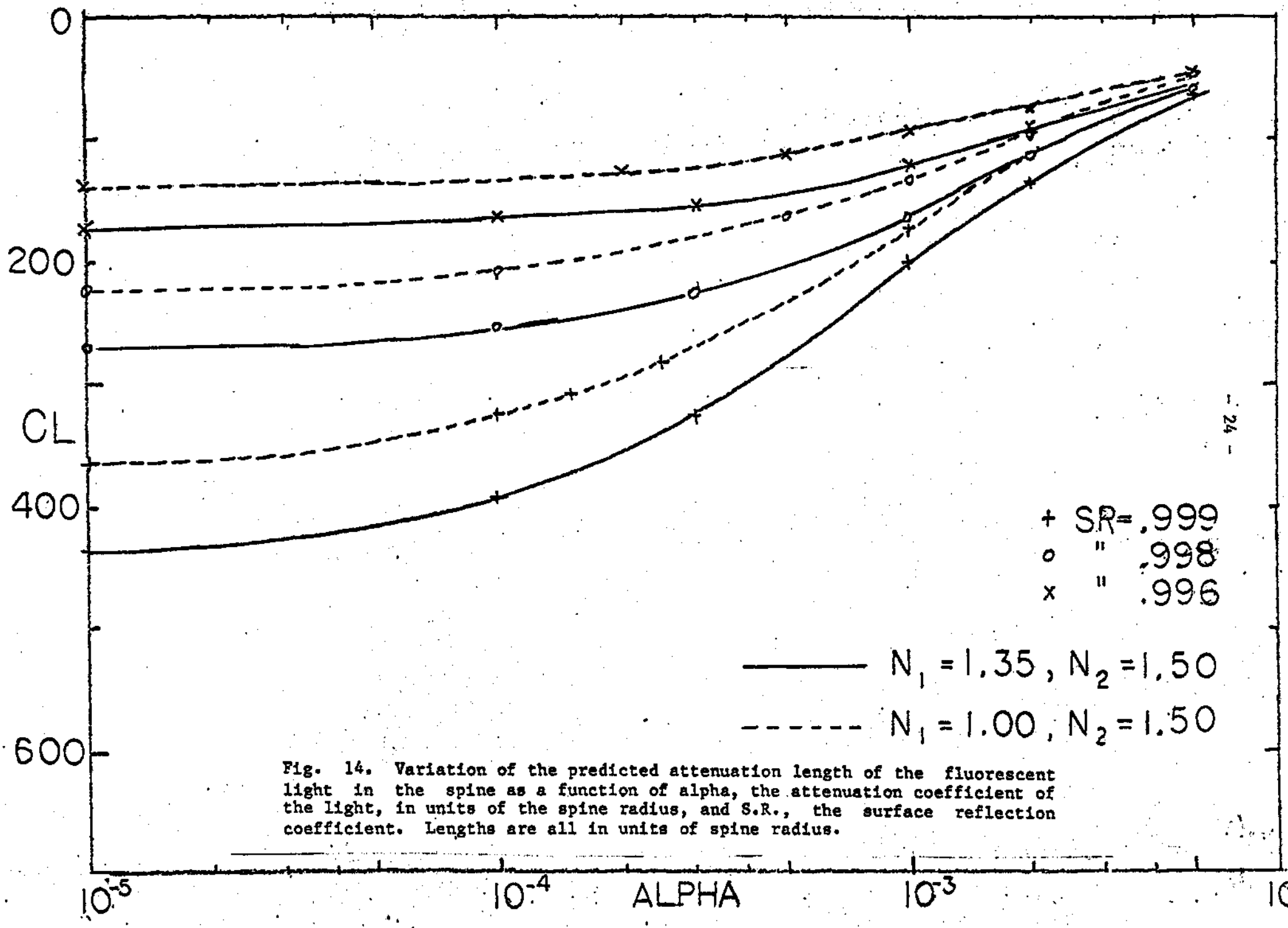

Fig. 14. Variation of the predicted attenuation length of the fluorescent light in the spine as a function of alpha, the attenuation coefficient of the light, in units of the spine radius, and S.R., the surface reflection coefficient. Lengths are all in units of spine radius.

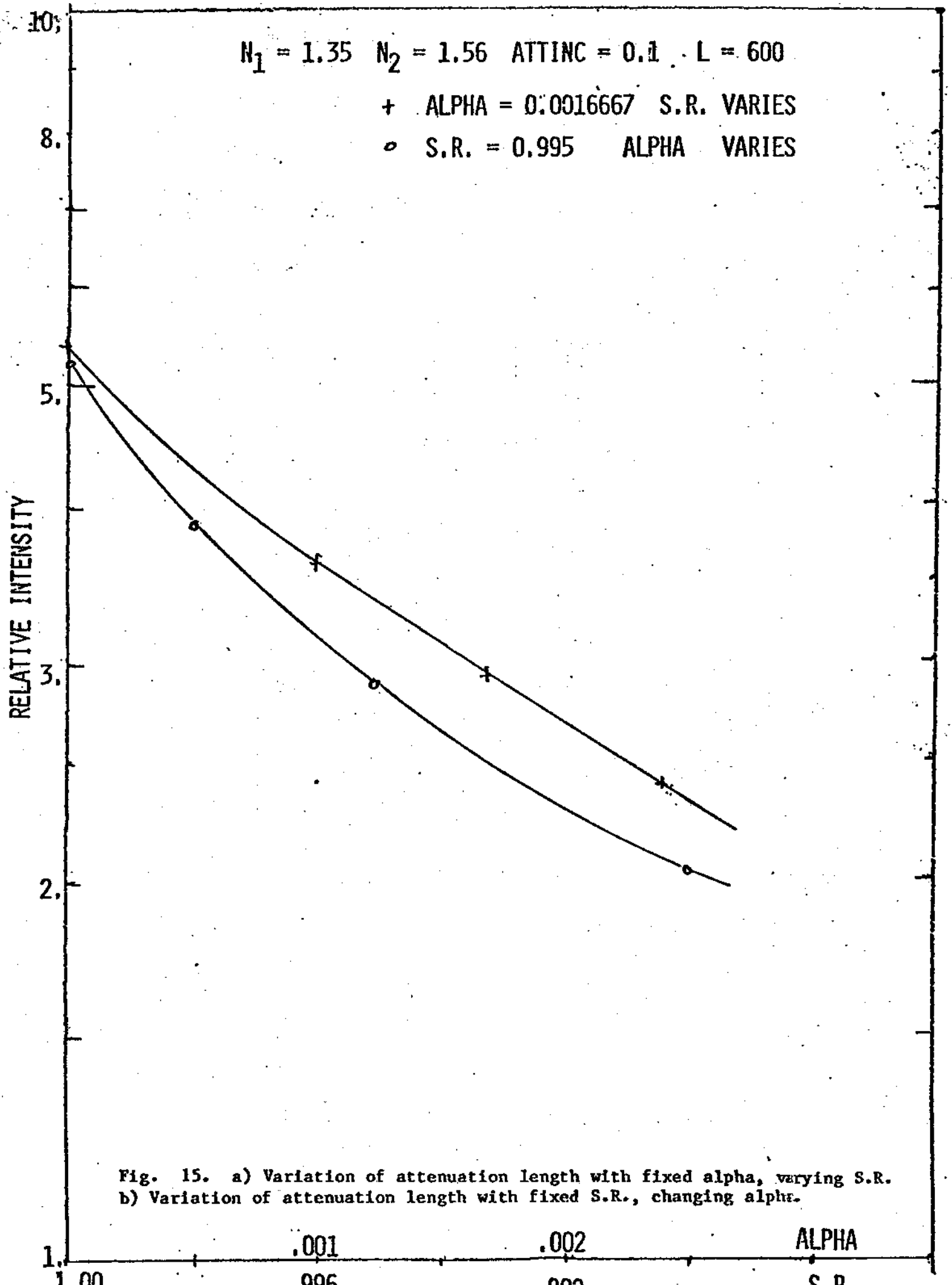

Fig. 15. a) Variation of attenuation length with fixed alpha, varying S.R.
b) Variation of attenuation length with fixed S.R., changing alpha.

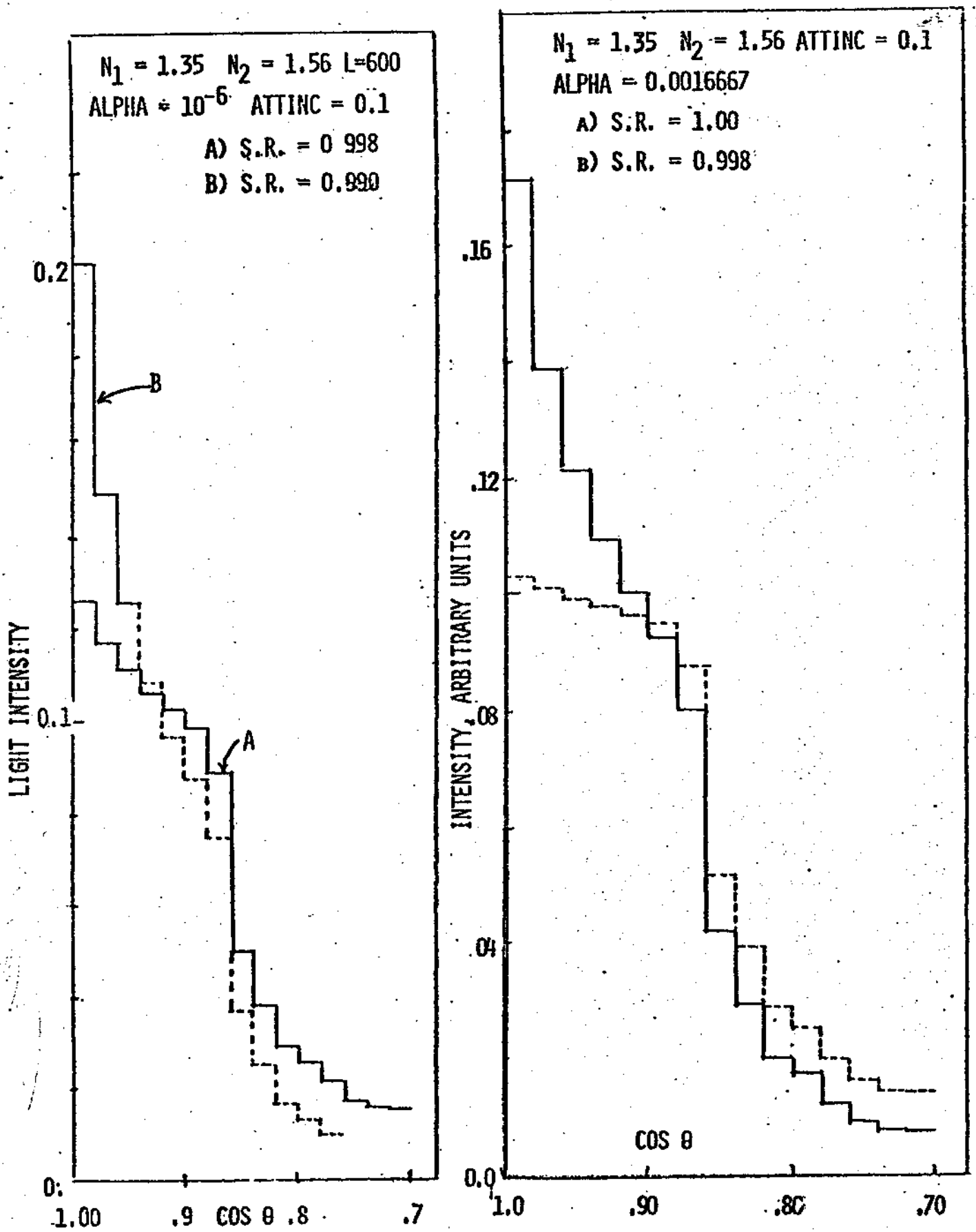

Fig. 16. a.) Predicted angular distribution of the light reaching the end of the spine at the PMT (in a medium of the same index of refraction as the spine) These curves are for alpha = 0, S.R. variable. b.) Same, for a moderate value of alpha, S.R. variable. Note how the cone narrows with increasing attenuation.